

Measurements of inclusive and differential Higgs boson production cross sections at 13.6TeV in the $H \rightarrow \gamma\gamma$ decay channel

Chen Zhou, Chengyang Pan

Peking University

2024.11.14



Motivation

- Determine the Higgs properties and test the Higgs compatibility with the standard model (SM) predictions.
- Measure the fiducial cross sections of Higgs boson production.
- First $H \rightarrow \gamma\gamma$ result with Run3 data @ 13.6TeV in CMS.

- Signal modelling: ggH, VBF, VH and ttH.
- Three mass points are used: 120GeV, 125GeV, 130GeV
- Optimisation of categories: diphoton and $\gamma + \text{jets}$.
- Corrections: Drell-Yan sample.
- Data: 2022 dataset=34.7/fb.

Photon selection and identification

- Preselections:
 - Requirements on p_T^γ , η_{SC} , photon ID, and shower shape and isolation observables to match the HLT requirements.
- ID:
 - Optimised cut at MVA score > 0.25 .

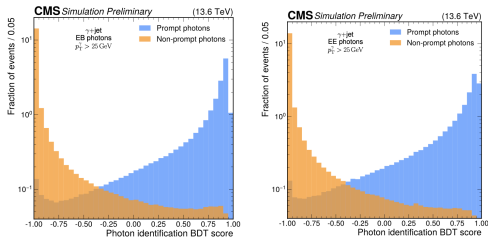


Fig. 1: Normalised distributions of the photon identification BDT scores for Barrel(left) and Endcap(right)

Photon scale and smearing corrections

- Residual shift in the photon energy scale between data and MC.
- $Z \rightarrow ee$ electrons are reconstructed as photons.

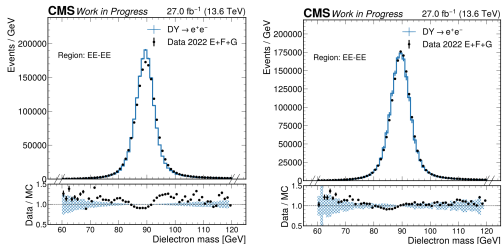


Fig. 2: EGamma Scale and Smearing corrections: before(left) and after(right)

Event categorisation

- Three categories are defined according to σ_m/m to enhance S/B. (With the MVA ID)

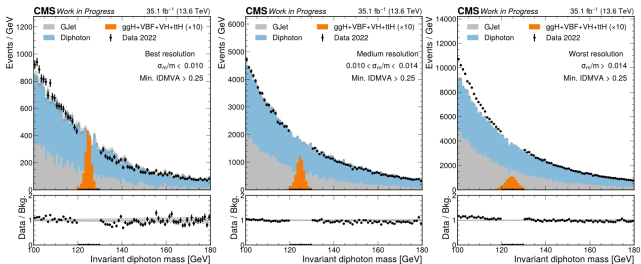


Fig. 3: Event categorisation

Correcting photon variables

- Photon mismodelling in the simulation is important.
- Shower shape and isolation observables (inputs to photon ID BDT), as well as the energy resolution are corrected with a novel method based on normalising flows. [paper](#)

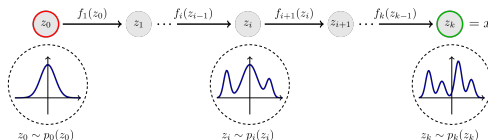


Fig. 4: Normalizing-flow

Correcting photon variables

- Flows achieve excellent data/MC agreement.
- The score of the photon ID MVA is reevaluated with the corrected input variables.
- The event categorisation based on the mass resolution is optimized .

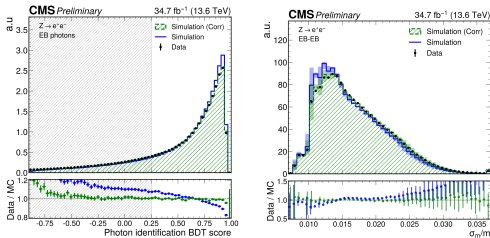


Fig. 5: BDT score and energy resolution after correcting

Jet definition and Fiducial phase space

- Jet definition:
 - Anti- κ_T clustering of stable particle.
 - Jets cleaning:
 - Distance parameter: $\Delta R < 0.4$. (With both photon and electron, muon)
 - Electrons: $p_T^e > 15\text{GeV}$, $|\eta^e| < 2.5$, $I < 0.2$.
 - Muon: $p_T^\mu > 10\text{GeV}$, $|\eta^\mu| < 2.4$, $I < 0.2$.
 - Add jet veto map: signal efficiency reduce by 1.5%.
 - Matches jet definition at reco level.
- Fiducial phase space:
 - $p_T^\gamma > 10\text{GeV}$ and $|\eta^\gamma| < 2.5$.
 - $1.4442 < |\eta^\gamma| < 1.566$ region is masked.
 - $\text{Iso} = \sum_i^{\text{R} < 0.3} \frac{p_{T,i}}{p_T} \times p_T^\gamma < 10\text{GeV}$.
 - $\sqrt{p_T^{\gamma 1} p_T^{\gamma 2}} / m_{\gamma\gamma} > 1/3$ and $p_T^{\gamma 2} / m_{\gamma\gamma} > 1/4$.

The statistical model and Systematic uncertainties

$$\mathcal{L}(\vec{\mu}, \vec{\theta}, m_H) = \prod_c \prod_b^{\text{kinBins}} \text{Pois} \left[n_{\text{obs}} \mid \sum_j^{\text{genBin}} \mu_j^{\text{fid}} S_j(\vec{\theta}, m_H) f_S(\vec{\theta}, m_H) + N^{\text{out}}(\vec{\theta}) f_S^{\text{out}}(\vec{\theta}, m_H) + B(\vec{\theta}) f_B(\vec{\theta}) \right] \times \prod_{k=1}^{n_k} p_k(\vec{\theta}_k \mid \theta_k)$$

- $S = (\epsilon \cdot A) \cdot L \cdot \sigma \cdot BR$.
- Contribution from events outside of the fiducial phase space.
- Contribution from the background modelling.
- Including experimental and theoretical uncertainties.

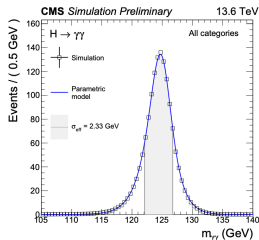


Fig. 6: Signal modelling

Inclusive fiducial cross section

- $\sigma_{fid} = 78 \pm 11(stat.)_{-5}^{+6}(syst.)fb = 78_{-12}^{+13}fb$
- Comparison with ATLAS result.
 - $\sigma_{fid}^{ATLAS} = 76 \pm 11(stat.) \pm 6(syst.)fb = 76 \pm 13fb$
- In agreement with SM prediction.
($67.8 \pm 3.8fb$)

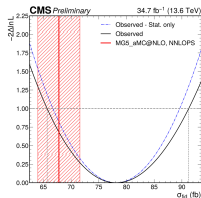


Fig. 7: Inclusive fiducial cross section

Impacts and Bin boundaries

- Dominated by energy scale and resolution.

Systematic uncertainty	Magnitude
Photon energy scale and resolution group	+5.8% / - 4.9%
Category migration from energy resolution	+3.5% / - 3.9%
Integrated luminosity	±1.4%
Photon preselection efficiency	±1.4%
Energy scale non-linearity	+0.8% / - 1.6%
Photon identification efficiency	±1.0%
Pileup reweighting	±0.8%

Fig. 8: Impacts on fiducial inclusive results

Observable	Binning	0	15	30	45	80	120	200	350	∞
p_T^H	0	0	0.15	0.3	0.6	0.9	2.5			
$ y^H $	0	0	0.15	0.3	0.6	0.9	2.5			
N_{jets}	0	0	1	2	3	4	∞			

Fig. 9: Bin boundaries for the differential cross sections.

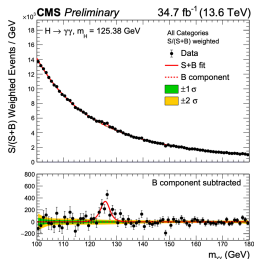
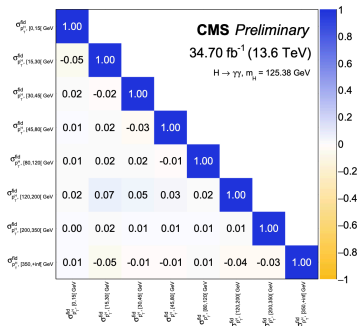
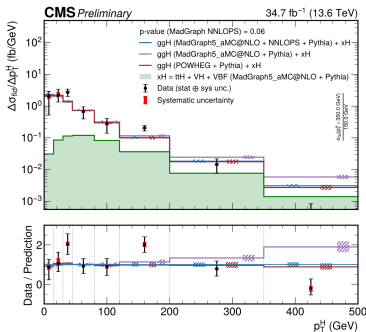


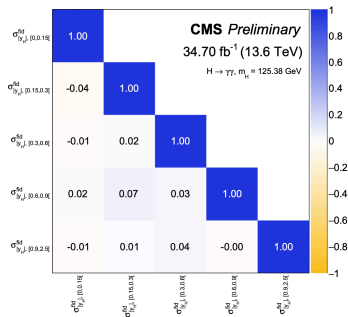
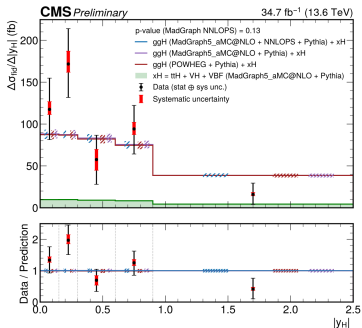
Fig. 10: Diphoton invariant mass distribution

Differential fiducial cross section: pTH



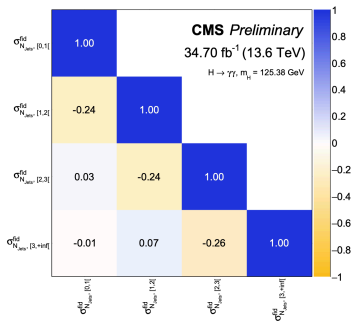
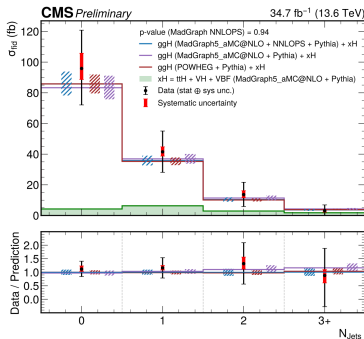
- Spectrum and correlation matrix for the transverse momentum of the Higgs boson.
- Agreement with SM prediction.

Differential fiducial cross section: rapidity



- Spectrum and correlation matrix for the absolute value of the rapidity of the Higgs boson.
- Agreement with SM prediction.

Differential fiducial cross section: number of jets



- Spectrum and correlation matrix for the absolute value of the number of associated jets.
- Nice agreement with SM prediction.

Summary

- First CMS Higgs result in Run 3, important validation of Run 3 performance. [PAS link](#)
- New method to correct photon observables using normalising flows.
 - Correct all ingredients for BDT and mass resolution.
- Fiducial inclusive and differential cross sections.
 - In agreement with SM prediction.

Back Up

From miniAOD to NanoAOD

- The mass resolution in the $H \rightarrow \gamma\gamma$ is driven by:
 - photon energy resolution.(ECAL)
 - precision measurement of the opening angle between the two photons.(vertex choice)
- $H \rightarrow \gamma\gamma$ vertex previously assigned by means of a BDT and all MiniAOD variables were recomputed wrt to the chosen diphoton vertex.
- Hgg vertex cannot be used with central NanoAOD \rightarrow private NanoAOD.

Normalizing flows

- Train a single normalizing flow on both MC and data simultaneously.
- Events are conditioned on an "IsData" boolean, which allows the flow to learn both distributions.

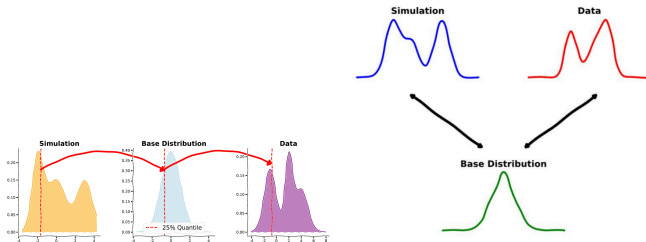


Fig. 11: The normalizing flows

Fraction of out-of-fiducial events

$$\mathcal{L}(\vec{\mu}, \vec{\theta}, m_H) = \prod_c^{\text{cat}} \prod_b^{\text{kinBins}} \text{Pois} \left[n_{\text{obs}} \mid \sum_j^{\text{genBin}} \mu_j^{\text{fid}} S_j(\vec{\theta}, m_H) f_S(\vec{\theta}, m_H) + N^{\text{out}}(\vec{\theta}) f_S^{\text{out}}(\vec{\theta}, m_H) + B(\vec{\theta}) f_B(\vec{\theta}) \right] \times \prod_{k=1}^{n_k} p_k(\vec{\theta}_k | \theta_k)$$

Fraction of out-of-fiducial events

	Best resolution	Medium resolution	Worst resolution
ggH	0.06%	0.19%	1.62%
VBF	0.17%	0.50%	1.97%
VH	0.31%	0.57%	2.16%
ttH	0.57%	0.83%	2.30%

- Consider photons in acceptance with $p_T > 25\text{GeV}$.
- Apply BDT to reduce background.
- Retain the $p_T^{\gamma\gamma}$ -leading diphoton system if $p_T^{\gamma 1} > 35\text{GeV}$.

Category	R9	H / E	sieie	Hollow cone track isolation	PF photon isolation
Barrel, high R9	> 0.85	< 0.08	–	–	–
Barrel, low R9	$[0.5, 0.85]$	< 0.08	< 0.015	$< 6\text{ GeV}$	$< 4\text{ GeV}$
Endcap, high R9	> 0.9	< 0.08	–	–	–
Endcap, low R9	$[0.8, 0.9]$	< 0.08	< 0.035	$< 6\text{ GeV}$	$< 4\text{ GeV}$